



**HAL**  
open science

## Sorption and Redox Speciation of Plutonium at the Illite Surface

Nidhu Lal Banik, Remi Marsac, Johannes Lützenkirchen, Alexandre Diascorn, Kerstin Bender, Christian M. Marquardt, Horst Geckeis

► **To cite this version:**

Nidhu Lal Banik, Remi Marsac, Johannes Lützenkirchen, Alexandre Diascorn, Kerstin Bender, et al.. Sorption and Redox Speciation of Plutonium at the Illite Surface. *Environmental Science and Technology*, 2016, 50 (4), pp.2092 - 2098. 10.1021/acs.est.5b05129 . hal-01904367

**HAL Id: hal-01904367**

**<https://hal.science/hal-01904367>**

Submitted on 24 Oct 2018

**HAL** is a multi-disciplinary open access archive for the deposit and dissemination of scientific research documents, whether they are published or not. The documents may come from teaching and research institutions in France or abroad, or from public or private research centers.

L'archive ouverte pluridisciplinaire **HAL**, est destinée au dépôt et à la diffusion de documents scientifiques de niveau recherche, publiés ou non, émanant des établissements d'enseignement et de recherche français ou étrangers, des laboratoires publics ou privés.

# Sorption and Redox Speciation of Plutonium at the Illite Surface

Nidhu lal Banik<sup>‡\*</sup>, Rémi Marsac<sup>‡†</sup>, Johannes Lützenkirchen<sup>‡</sup>, Alexandre Diascorn<sup>‡#</sup>, Kerstin  
Bender<sup>‡</sup>, Christian Michael Marquardt<sup>‡</sup> and Horst Geckeis<sup>‡</sup>

<sup>‡</sup>Institut für Nukleare Entsorgung, Karlsruhe Institute of Technology, P.O. Box 3640, D-76021  
Karlsruhe, Germany

**ABSTRACT.** The geochemical behavior of Pu strongly depends on its redox speciation. In this study we investigated Pu sorption onto Na-illite, a relevant component of potential host rocks for high-level nuclear waste repositories, under anaerobic conditions. When contacting Pu (85% Pu(IV), 11% Pu(V) and 4% Pu(III);  $8 \times 10^{-11} < [\text{Pu}]_{\text{tot}}/M < 10^{-8}$ ) with illite in 0.1 M NaCl at pH between 3 and 10, Pu uptake was characterized by  $\log R_d > 4$  ( $R_d$ : distribution coefficient in  $\text{L kg}^{-1}$ ). Small amounts of aqueous Pu(V) were detected in solution on contact with illite after one week which is not expected to be stable at the measured redox potentials (Eh) in our experiments. This observation suggests time dependent reduction of Pu(V) to Pu(IV). After one year,  $\log R_d$  values had increased compared to those after one week due to the reduction of weakly adsorbing Pu(V). For  $\text{pH} < 5$ , Pu(IV) and Pu(III) coexisted in solution under our experimental conditions, showing that Pu(IV) reduction to Pu(III) occurred in the illite suspension. Taking (i) surface complexation constants determined for Eu(III)-illite interaction (with redox insensitive Eu(III) as a chemical analogue to Pu(III)), (ii) the known constant for Pu(III)/Pu(IV) redox transition, and (iii) measured Eh and pH, overall Pu uptake was well predicted.

## 22 INTRODUCTION

23 Due to its high radiotoxicity and the very long half-lives of some isotopes, plutonium (Pu) is an  
24 important element in the context of nuclear waste disposal. Under environmentally relevant  
25 conditions, Pu can occur in the oxidation states +III, +IV, +V and +VI. As the geochemical  
26 behavior of Pu, such as solubility and mobility, strongly depends on its redox state,<sup>1,2</sup>  
27 thermodynamic speciation calculations need to account for Pu redox speciation.

28 Several studies have shown that actinide redox chemistry is affected by interaction with mineral  
29 surfaces. The evaluation of Pu sorption data is particularly challenging as frequently a mixture of  
30 Pu redox states is found in solid/liquid systems (i.e. at the surface and/or in solution). In the  
31 presence of a mineral, rates for abiotic redox reactions range from a few hours to a few months  
32 and depend on the mineral type, pH, Pu concentration and initial Pu redox state, which further  
33 complicates data interpretation.<sup>3-8</sup> Generally, under ambient (air) atmosphere, when adding  
34 Pu(IV), Pu(V) or Pu(VI) to a mineral suspension (hematite, goethite, magnetite,<sup>5-10</sup> quartz,<sup>11</sup>  
35 montmorillonite,<sup>3,4</sup> kaolinite<sup>12</sup>), Pu(IV) is found at the mineral surface whereas very often Pu(V)  
36 prevails in solution. Similar observations were made for neptunium (Np) and illite under slightly  
37 reducing conditions.<sup>13</sup> However, the standard redox potential of the Np(V)/Np(IV) couple  
38 ( $E_{NpO_2^+/Np^{4+}}^0 = 0.604 V$ ) is lower than that of the Pu(V)/Pu(IV) pair ( $E_{PuO_2^+/Pu^{4+}}^0 = 1.031 V$ ).<sup>14</sup>  
39 Pu sorption to minerals under reducing conditions, where Pu(III) should prevail, has been probed  
40 less frequently. Under inert (N<sub>2(g)</sub> or Ar<sub>(g)</sub>) atmosphere, magnetite was shown to reduce Pu(V) to  
41 Pu(III) at pH = 6 and 8, whereas Pu(III) was not observed under ambient atmosphere.<sup>7,15</sup> In the  
42 presence of kaolinite and NH<sub>2</sub>OH·HCl added as a weaker reducing agent than magnetite, Pu(III)  
43 was oxidized to Pu(IV) at pH > 6.<sup>16</sup> Banik et al.<sup>13</sup> noticed the presence of Pu(III) at pH = 1 in the  
44 solution when in contact with kaolinite under ambient atmosphere, which is explained by the

45 higher stability of Pu(III) at low pH. All these studies suggest that Pu redox speciation is strongly  
46 affected by the redox conditions in the investigated system and the presence of mineral surfaces.  
47 In recent studies, it was shown that the overall uptake of redox sensitive actinides can be  
48 quantitatively predicted by taking into account the uptake of the individual redox states and the  
49 measured redox potentials, i.e. the negative logarithm of (apparent) electron activity,  $p_e$ . In the  
50 case of Np, the high stability of Np(IV) surface complexes significantly extended the  
51 predominance field of Np(IV) at the illite surface as compared to that valid for the pure aqueous  
52 solution. This finding explains the prevalence of Np(V) in solution and of Np(IV) at the surface.  
53 Overall  $R_d$  values obtained for the sorption of Np thus lie between that of penta- and tetravalent  
54 actinides.<sup>13</sup> The same modeling approach was applied to simulate Pu sorption and redox  
55 speciation at the kaolinite surface.<sup>17</sup> Lanthanides and actinides are known to exhibit similar  
56 chemical behavior for a given redox state.<sup>1,2,18</sup> Because separate uptake data for the four distinct  
57 Pu redox states are not available (and will be difficult to obtain experimentally), sorption data for  
58 europium(III) or americium(III) ( $\text{Eu}^{3+}/\text{Am}^{3+}$ ), thorium(IV) ( $\text{Th}^{4+}$ ), neptunium(V) ( $\text{NpO}_2^+$ ) and  
59 uranium(VI) ( $\text{UO}_2^{2+}$ ) were used to estimate sorption data of the respective Pu redox states. As  
60 both Pu(IV) and Pu(III) show strong sorption to mineral surfaces over a wide range of pH  
61 conditions, Pu(IV) and Pu(III) predominance fields are expected to be less affected by the  
62 presence of mineral surfaces than in the case of Np,<sup>13,17</sup> where the sorption behavior of the redox  
63 species +V and +IV are clearly different.

64 Pu sorption onto purified illite<sup>13</sup> in 0.1 M NaCl is experimentally investigated in the present study  
65 under anaerobic conditions in order to verify the reliability and applicability of those previously  
66 reported modeling approaches. Pu sorption to illite is interpreted involving known data on redox  
67 and adsorption equilibria within the 2 site protolysis non-electrostatic surface complexation and  
68 cation exchange (2 SPNE SC/CE) model<sup>19-21</sup> to quantify Pu surface speciation.

## 69 MATERIALS AND METHODS

70 All chemicals (pro analytical quality or better) were obtained from Merck (Darmstadt, Germany)  
71 or Riedel de Haen (Seelze, Germany). Solutions were prepared with de-ionized “MilliQ” water  
72 (specific resistivity,  $18.2 \text{ M}\Omega \text{ cm}^{-1}$ ). The purified Na-illite was provided within the EC project CP  
73 CatClay ([www.catclay.org](http://www.catclay.org)). The source material derives from lacustrine continental sediments  
74 deposited at the Upper Eocene ( $\sim -35 \text{ Ma}$ ) in the basin of Le Puy en Velay (Massif Central,  
75 France). The purification procedures and the characterization of the purified illite ( $<63 \mu\text{m}$ ) were  
76 previously given in detail<sup>13</sup> and will not be repeated here. Note that in the last step of the  
77 purification, the clay suspension was freeze dried, to exclude bacterial activity.

78  
79 **Plutonium and Europium stock solution.** A  $^{238}\text{Pu}$  stock solution was prepared from a  
80 solution of plutonium dissolved in concentrated nitric acid, which was fumed three times by 0.1  
81 M  $\text{HClO}_4$ , in order to remove nitrate and organic traces. The concentration of the Pu stock  
82 solution was  $3.9 \times 10^{-5} \text{ M}$  in 0.1 M  $\text{HClO}_4$ . A more dilute solution ( $[\text{Pu}] = 1.9 \times 10^{-6} \text{ M}$ ) in 0.1 M  
83  $\text{HClO}_4$  was prepared from that stock solution – however, the solution was left under argon  
84 atmosphere for several months before dilution - to perform experiments at low Pu(IV)  
85 concentration. The concentrations of  $^{238}\text{Pu}$  in solution were determined by liquid scintillation  
86 counting (LSC) using the scintillation cocktail Ultima Gold XR with a liquid scintillation  
87 analyzer (Tri-Carb 3110TR). In addition, the stock solution of  $^{238}\text{Pu}$  were checked by ICP-MS  
88 measurements and the results were in excellent agreement with LSC measurements.

89 Eu(III) was investigated as a chemical analogue of Pu(III). A radiotracer solution was purchased  
90 from Amersham International (total Eu concentration:  $6.0 \times 10^{-4} \text{ M}$ ) with isotopic composition:  
91  $^{151}\text{Eu}$  (83%),  $^{152}\text{Eu}$  (13%,  $t_{1/2} = 13.33\text{a}$ ),  $^{153}\text{Eu}$  (4%).  $^{152}\text{Eu}$  is a  $\beta$ -,  $\gamma$ -emitter and can be

92 conveniently analyzed by  $\gamma$ -counting. In the present study, precise determination of dissolved  
93  $^{152}\text{Eu}$  concentration, was performed using a Perkin Elmer Wallac gamma counter (Wizard 1480).  
94

95 **Plutonium redox state analysis by liquid-extraction methods.** The Pu redox state  
96 distribution in the diluted  $^{238}\text{Pu}$  stock solution ( $1.9 \times 10^{-6}$  M; in 0.1 M  $\text{HClO}_4$ ) and in the  
97 supernatant of Pu-illite samples prepared for  $[\text{Pu}]_{\text{tot}} = 10^{-8}$  M was determined by liquid-liquid  
98 extraction.<sup>22,23</sup> Two different complexing agents, 0.025 M PMBP in toluene and 0.5 M HDEHP in  
99 xylene, were used (PMBP: 4-benzoyl-3-methyl-1-phenyl-pyrazolin-5-one; HDEHP: phosphoric  
100 acid bis-(2-ethyl-hexyl) ester).<sup>22,23</sup> The aqueous Pu-sample solution mixed with the organic  
101 extractant was stirred for 10 minutes and then centrifuged for 10 minutes at 4000 rounds per  
102 minute (rpm). After separation of the aqueous and the organic phases, activities were measured in  
103 each phase by LSC. Four different extractions were made separately. With PMBP at pH 0  
104 (extraction 1), Pu(IV) is extracted into the organic phase, while Pu(III), Pu(V), Pu(VI) and  
105 polymers remain in the aqueous phase. With PMBP at pH 0 and 0.02 M  $\text{Cr}_2\text{O}_7^{2-}$  (extraction 2),  
106 Pu(III) and Pu(IV) are extracted into the organic phase, while Pu(V), Pu(VI) and polymers  
107 remain in the aqueous phase. With HDEHP at pH 0 (extraction 3), Pu(IV) and Pu(VI) are  
108 extracted into the organic phase, while Pu(III), Pu(V) and polymers remain in the aqueous phase.  
109 With HDEHP at pH 0 and 0.02 M  $\text{Cr}_2\text{O}_7^{2-}$  (extraction 4), Pu(III), Pu(IV), Pu(V) and Pu(VI) are  
110 extracted into the organic phase while polymers remain in the aqueous phase. All steps for the  
111 separation of the different oxidation states of plutonium and the calculation leading to the  
112 aqueous redox speciation of Pu are outlined in the supporting information (Figure S1). The  
113 uncertainty of the method is conservatively estimated to be  $\pm 10\%$ , and includes the pipetting  
114 error, phase separation of mixture, quenching factor of the analyte solution (color) for the LSC

115 measurements and the variability observed for different extraction experiments. The diluted  $^{238}\text{Pu}$   
116 stock solution contained 85% Pu(IV), 11% Pu(V) and 4% Pu(III). Seemingly, the Pu(VI)  
117 expected from the preparation step is not stable at low concentrations under the present  
118 experimental conditions, which was also observed by Neck et al.<sup>24</sup>

119  
120 **Determination of pH and Eh.** The pH in the clay suspensions was measured by an Orion  
121 525A (pH meter) and a Ross electrode calibrated with 4 standard buffers (pH 3, 5, 7 and 9;  
122 Merck). The error in pH measurements is  $\pm 0.05$ . The redox potentials in the clay suspensions  
123 were measured using an Orion 525A ( $E_h$  meter) and a Pt electrode combined with the Ag/AgCl  
124 reference system (Metrohm). Raw data were converted into  $E_h$  vs. standard hydrogen electrode  
125 (SHE) by correcting for the potential of the reference electrode.  $E_h$  was converted to the apparent  
126 electron activity,  $p_e = -\log a_{e^-} = 16.9 \times E_h(\text{V})$  at 25°C. A commercial redox-buffer (220 mV,  
127 Schott instruments) was used for calibration. After having stirred the suspension, a time span of  
128 15 min was allowed for all  $E_h$  measurements. Uncertainties in  $E_h$  measurements are  $\pm 50$  mV.<sup>15,24</sup>

129  
130 **Batch sorption experiments.** All sorption studies were performed as batch type  
131 experiments. The effect of pH was investigated for an initial Pu concentration ( $[\text{Pu}]_{\text{tot}}$ ) of  $8 \times 10^{-11}$   
132 M. In addition, the effect of  $[\text{Pu}]_{\text{tot}}$  was investigated for  $8 \times 10^{-11} < [\text{Pu}]_{\text{tot}} < 10^{-8}$  M, at pH  $\approx 4, 7$   
133 and 10. Batch experiments were carried out in 40 mL polypropylene centrifuge tubes at room  
134 temperature in an argon glove box ( $< 1$  ppm  $\text{O}_2$ , absence of  $\text{CO}_2$ ). The suspension volume was 25  
135 mL. At a solid to liquid ratio of  $2 \text{ g L}^{-1}$ , the suspensions were preconditioned in 0.1 M NaCl  
136 under continuous shaking for 4-5 days to achieve a given target pH value by adding 0.1 M HCl or  
137 0.1 M NaOH. After adding Pu to the illite suspension, pH was adjusted again to the required pH

138 of the sample. Neither pH nor Eh buffers were used. The samples were closed and shaken end-  
139 over-end. After one week, pH and Eh were measured in the suspension and an aliquot of each  
140 sample was transferred to special centrifuge tubes (Beckmann, Recorder No.: 356562) and  
141 centrifuged (Beckmann Coulter XL-90 K) at 90,000 rpm (~700,000 g max) for one hour. The  
142 supernatant was analyzed for dissolved Pu by LSC. Samples were kept in the glovebox without  
143 any pH adjustment and the procedure was repeated after one year of contact time. Results from  
144 the batch experiments are expressed throughout as distribution coefficients ( $R_d$  in  $L\ kg^{-1}$ ),  
145 calculated by the following equation:

146

$$147 \quad R_d = ([Pu]_{tot}/[Pu]_{aq} - 1) \times V/m \quad (1)$$

148

149 where  $[Pu]_{aq}$  and  $[Pu]_{tot}$  (M) are the dissolved (final) equilibrium and total (initial) concentrations  
150 of Pu, respectively. The term  $V/m$  corresponds to the aqueous solution volume to illite mass ratio  
151 ( $L\ kg^{-1}$ ). According to our experimental results (see below), an uncertainty of  $\pm 0.2$  (standard  
152 deviation) is assigned to  $\log R_d$ , although it could be larger according to comparable studies  
153 where more than 99% uptake is obtained.<sup>20,21</sup> Under such conditions, larger uncertainties are  
154 induced by analytical constraints.

155 Batch Eu sorption experiments were performed for  $[Eu]_{tot} = 3 \times 10^{-9}$  M applying the same protocol  
156 as for Pu, except that Eh was not recorded because Eu is not redox sensitive under our  
157 experimental conditions. After one week contact time and subsequent ultracentrifugation, the  
158 supernatant was analyzed for dissolved Eu by  $\gamma$ -spectrometry. The latter procedure was repeated  
159 after 4 months to estimate potential aging effects on Eu sorption to illite. No aging effect is  
160 observed for Eu(III) under our experimental conditions (see Fig. S2).



161  
162 **Thermodynamic modeling.** pe-pH diagrams for Pu were constructed using PhreePlot,<sup>25</sup>  
163 which contains an embedded version of the geochemical speciation program PHREEQC.<sup>26</sup>  
164 Thermodynamic constants for Pu and Eu aqueous speciation were taken from the NEA  
165 thermodynamic database.<sup>14</sup> The specific ion interaction theory (SIT)<sup>27</sup> was used for the  
166 calculation of the activity coefficients of aqueous species. In case of gaps in the Pu database, data  
167 for analogues were chosen (i.e. Eu(III), Np(IV), Np(V) and U(VI) for the respective Pu redox  
168 states). Auxiliary reactions and constants (from the SIT database) are provided with PHREEQC  
169 (sit.dat file). The 2 SPNE SC/CE model was used to simulate Pu and Eu sorption to illite, where  
170 the cation exchange capacity (CEC) and the strong site density of the illite surface are considered  
171 equal to 0.225 eq kg<sup>-1</sup> and 2×10<sup>-3</sup> mol kg<sup>-1</sup>, respectively.<sup>19-21</sup> Only the strong sites within the 2  
172 SPNE SC/CE model are considered in the adsorption calculations. The weak sites play a  
173 negligible role in our experiments, since a maximum Pu loading of only 5×10<sup>-6</sup> mol kg<sup>-1</sup> (i.e. for  
174 [Pu]<sub>tot</sub> = 10<sup>-8</sup> M) is investigated. A complete summary of the thermodynamic database, SIT  
175 coefficients and parameters for the 2SPNE SC/CE model is given in the supporting information  
176 (Table S1, S2 and S3).

177  
178 **RESULTS AND DISCUSSION**

179 **Pu sorption to illite in 0.1 M NaCl.** pH-pe data recorded after 1 week and 1 year  
180 equilibration time in the Pu-illite suspension in 0.1 M NaCl solution are plotted in Figure 1  
181 together with the calculated predominance pH-pe diagram for dissolved Pu. The solid lines  
182 correspond to equal amounts of two Pu redox states. Large symbols indicate the samples where  
183 the supernatant was additionally analyzed by liquid extraction ([Pu]<sub>tot</sub> = 10<sup>-8</sup> M; see Table S4 and

184 S5 for more information regarding these samples). Data are compared to those reported for the  
185 Np-illite system at similar metal ion concentration ( $3 \times 10^{-8}$  M) and after contact times between 7  
186 and 63 days<sup>13</sup> and agree well within experimental uncertainties. Between 1 week and 1 year, pH  
187 may slightly evolve due to further buffering of illite, since no pH-buffer was used. An increase in  
188 pe values is also observed for the batch series prepared to study the effect of pH ( $[\text{Pu}]_{\text{tot}} = 8 \times 10^{-11}$   
189 M), which is potentially due to the presence of undetectable traces of  $\text{O}_{2(\text{g})}$  (i.e. < 1 ppm) during  
190 sample handling or storage over the 1 year period. This has, however, no impact on our  
191 conclusions, which are based on the finally established pe and pH values. Batch series conducted  
192 for pH  $\approx$  4, 7 and 10 ( $8 \times 10^{-11} < [\text{Pu}]_{\text{tot}} < 10^{-8}$  M) exhibit quite stable pe values with time, which  
193 suggests no significant  $\text{O}_{2(\text{g})}$  contamination or microbial activity over the 1 year period.

194 Significant amounts of Pu(III) are expected in the aqueous phase below pH  $\approx$  5 whereas Pu(IV)  
195 should prevail above pH  $\approx$  6 according to the calculations and taking pe data uncertainties into  
196 account. However, in sorption experiments ( $[\text{Pu}]_{\text{tot}} = 10^{-8}$  M) performed over a period of 1 week,  
197 we found at pH = 4.3 about 90% of the Pu in the supernatant aqueous phase being pentavalent  
198 (Table S5). In analogy to the observed behavior of Np(V), the Pu(V) sorption to illite at pH = 4.3  
199 is considered negligible and remains in solution. Pu(IV), like other tetravalent actinide ions, is  
200 expected to be almost completely sorbed (see e.g. the literature Np(V)- and Th(IV)-illite sorption  
201 data in Fig. S2 and Fig. S3, respectively).<sup>21,28</sup> In our sample, only 7% of the total Pu remain in  
202 solution. Therefore, Pu(V) represents  $\sim$ 6% of the total Pu amount in the system, which  
203 corresponds to about half of Pu(V) initially present in the <sup>238</sup>Pu stock solution (11% of Pu(V)). At  
204 pH = 6.9, only 3% of Pu remain in solution after ultracentrifugation with 20% Pu(V), while at pH  
205 = 10 the redox state of Pu in solution is entirely +IV after 1 week. We attribute this finding to a  
206 time dependent Pu(V) reduction in our system which apparently accelerates with increasing pH.  
207 A similar time dependent reduction of Pu(V) to Pu(IV) was observed in presence of hematite and

208 goethite,<sup>6,8,9</sup> montmorillonite<sup>3,4</sup> and other minerals.<sup>3,11</sup> Reanalysis after 1 year revealed stronger  
209 Pu sorption and Pu redox states ( $[\text{Pu}]_{\text{tot}} = 10^{-8}$  M) in the aqueous phase are now in better  
210 agreement with thermodynamic considerations. At pH = 4.3,  $22 \pm 10\%$  Pu(III),  $85 \pm 10\%$  Pu(IV)  
211 and no Pu(V) is detected. According to the measured pe data range ( $6.2 \pm 0.9$ ), between 88% and  
212 100% of Pu(III) are predicted to exist in solution and 0-12% Pu(IV) which qualitatively agrees  
213 with the experimental results. At pH = 6.9 and 9.3, Pu(IV) clearly dominates and no significant  
214 amounts of Pu(V) or Pu(III) could be found, as calculated using the measured pe values. We have  
215 to emphasize that the observed time dependent redox reaction relates to only the initial Pu(V), i.e.  
216 a small fraction of the total Pu. The major Pu fraction is sorbed, either as Pu(III) or Pu(IV).  
217 However, those small variations have a significant impact on  $R_d$  values, as will be discussed  
218 below. It is also understood that the time for attaining overall equilibrium might be shorter than 1  
219 year. Such a long waiting period has been chosen in order to make sure that equilibrium has  
220 established similar to the procedure proposed in a previous Pu-montmorillonite sorption study.<sup>3</sup>  
221 Figure 2a shows Pu sorption to illite ( $R_d$ : distribution coefficient in  $\text{L kg}^{-1}$ ) as a function of pH  
222 after 1 week and 1 year contact time for  $8 \times 10^{-11} < [\text{Pu}]_{\text{tot}} < 10^{-8}$  M. While Pu uptake by illite is  
223 always high,  $R_d$  values after 1 week are lower for pH < 7 than after 1 year (except for some data  
224 at pH = 4.3, which will be discussed later). This is consistent with the disappearance of Pu(V),  
225 which sorbs weakly compared to Pu(IV) and Pu(III). Earlier studies dealing with Np(V)-illite  
226 interaction<sup>13</sup> revealed faster redox reactions and equilibrium was assumed to be established after  
227 1 week. However, under those pH/pe conditions, Np prevails in pentavalent state in solution  
228 according to measurements and geochemical calculations which makes Np different from Pu.  
229 Consequently,  $R_d$  values for Np are smaller than those observed for Pu, so that slight variations in  
230 redox have less impact on  $R_d$  values for Np as compared to those for Pu. Slow redox kinetics for  
231 Np can thus not be excluded but the error related to kinetics might have been negligible

232 compared to, for instance, experimental uncertainty on  $p_e$ . Other mechanisms such as  
233 incorporation reactions or sorption by secondary phases might also explain slow reaction rates.  
234 Such reactions have been reported for mineral phases with high surface dynamics such as calcite,  
235 apatite and brucite which can be estimated from known mineral dissolution rates (see e.g. <sup>2,29</sup>).  
236 By contrast, dissolution rates of clays (e.g., for smectite)<sup>30</sup> are slow and actinide incorporation in  
237 clays has rarely been observed in laboratory studies,<sup>2</sup> except at high pH (i.e.  $pH > 12$ )<sup>31</sup> or in  
238 coprecipitation studies.<sup>32</sup> Moreover, sorption of redox inactive radionuclides such as Eu(III) and  
239 Am(III) to clays is relatively fast and proceeds within less than 1 week.<sup>20,21</sup> For instance, as  
240 shown in Figure S2, Eu(III) sorption to illite does not evolve significantly between 1 week and 4  
241 months equilibration time. Although incorporation processes of Pu(III/IV/V) in illite cannot be  
242 entirely excluded for the 1 year old samples, they very likely play a minor role with respect to the  
243 increase in  $R_d$  with time compared to Pu(V) reduction to Pu(IV).  
244 Given the general agreement of results of thermodynamic calculations with experimentally  
245 determined Pu redox states in solutions in contact with illite for 1 year, we assume establishment  
246 of an overall equilibrium. Pu uptake by illite after 1 year contact time (Figure 2a) is characterized  
247 by a constant  $\log R_d = 5.2 \pm 0.2$  ( $1\sigma$ ) for  $pH > 5$ . Sorption of tetravalent elements onto minerals is  
248 reported to be widely insensitive to pH as for Sn(IV) and Th(IV) sorption to illite shown in  
249 Figure S3.<sup>20,21</sup> Pu sorption data ( $\log R_d$ ) for  $pH > 5$  are plotted in figure 2b against the logarithm  
250 of the final aqueous Pu concentration ( $\log [Pu]_{aq}$ ).  $[Pu]_{aq}$  in presence of illite is close to or below  
251 the solubility limit of Pu(IV) in equilibrium with  $PuO_{2(am,hydr)}$  (i.e.  $\log [Pu]_{aq} \approx -10.4$ , for  $pH >$   
252  $6$ ).<sup>24</sup> Precipitation of  $PuO_{2(am,hydr)}$  can thus be excluded. Figure 2b shows that  $\log R_d$  is  
253 independent of the total Pu concentration and does not vary with  $\log [Pu]_{aq}$  for  $pH > 5$ . This is in  
254 line with previous studies of Th(IV) sorption onto illite-containing argillaceous rocks (where  
255 illite was shown to be the major adsorbant), where an ideal Th(IV) sorption was observed for a

256 similar range of Th(IV) to clay concentration ratios for  $7 < \text{pH} < 8$ .<sup>33,34</sup> Lower sorption of Pu at  
257  $\text{pH} = 3$  (figure 2a) can be attributed to the prevalence of less sorbing Pu(III), which is more stable  
258 at low pH (Fig. 1). Different sorption behavior of tri- and tetravalent metal ions at such low pH is  
259 well known for e.g. Eu(III) and Th(IV).<sup>19-21</sup> Scattering  $R_d$  data obtained for  $\text{pH} = 4.3$  might  
260 suggest a concentration-dependent uptake of Pu (figure 2b). However, this is very unlikely  
261 because investigated surface coverages (between  $4 \times 10^{-8}$  and  $5 \times 10^{-6}$  mol of Pu per kg of illite) are  
262 below the saturation of any high affinity sites for illite, where an ideal sorption behavior has been  
263 evidenced for many metal ions (see e.g. Figure 2 in reference 13, and references therein). Instead,  
264  $\log R_d$  variations at  $\text{pH} = 4.3$  might be explained by the observed uncertainties of measured  $p_e$   
265 data close to the Pu(IV)/Pu(III) borderline in Fig. 1 and possible slight heterogeneities in illite  
266 samples (e.g. with regard to Fe(II)-content).  $\log R_d$  seems to increase with  $p_e$  (Fig. 2c),  
267 consistent with a transition between Pu(III) and Pu(IV), even though a clear conclusion is  
268 hampered by the relatively large uncertainty of measured  $p_e$  data. This observation will be  
269 supported by surface complexation modeling (see below).

270

271 **Modeling results.** As previously found for Np(V) interaction with illite and Pu sorption to  
272 kaolinite and hematite, the redox speciation of actinides is influenced by the formation of surface  
273 complexes.<sup>13,17,35</sup> Equation 2 provides a simple approach to determine the stability field of Pu(IV)  
274 and Pu(III) at a mineral surface:<sup>17</sup>

275

$$276 \quad \{Pu(IV)/Pu(III)\}_{surf} = \{Pu(IV)/Pu(III)\}_{aq} + (\log R_d(Pu(III)) - \log R_d(Pu(IV))) \quad (2)$$

277

278  $\{\text{Pu(IV)/Pu(III)}\}_{\text{aq}}$  can be calculated by the Nernst equation (see reference 17 for details) and the  
279 redox borderline in aqueous solution (Figures 1 and 3a) denotes an equimolar Pu(III)/Pu(IV)  
280 ratio.  $\{\text{Pu(IV)/Pu(III)}\}_{\text{surf}}$  refers to the corresponding redox speciation at the illite surface. Log  
281  $R_d(\text{Pu(III)})$  and  $\log R_d(\text{Pu(IV)})$  values in eq. 2 represent the respective individual uptake of the  
282 two Pu redox states under the same physico-chemical conditions and are expressed as distribution  
283 coefficients (denoted as  $K_d$  in reference 17). As  $R_d$  values for Pu(III) and Pu(IV) are difficult to  
284 determine separately, we took in a first approach existing models for Eu(III)<sup>19</sup> and Np(IV)<sup>13</sup> to  
285 estimate sorption of Pu(III) and Pu(IV), respectively. The resulting Pu(IV)/Pu(III) borderline is  
286 shown in Figure 3a as a dashed bold red line. pH-edges for Eu(III) and Np(IV) sorption onto illite  
287 in 0.1 M NaCl calculated with the 2 SPNE SC/CE model are shown in Figure 3b. For pH < 7,  
288 Eu(III) sorption to illite is weaker than that of Np(IV). At this low pH outer-sphere sorption (ion  
289 exchange) dominates for Eu(III). Due to the higher thermodynamic stability of actinide(IV)  
290 surface complexes in this area, the predominance field of Pu(IV) is enlarged at the illite surface  
291 and overlaps with the stability field of Pu(III) in the aqueous phase. For pH > 7, Eu(III) and  
292 Np(IV) uptake are almost equal. As a consequence, the Pu(IV)/Pu(III) borderline at the illite  
293 surface coincides with that in solution ( $\{\text{Pu(IV)/Pu(III)}\}_{\text{surf}} \approx \{\text{Pu(IV)/Pu(III)}\}_{\text{aq}}$ ). The pH-pe  
294 values measured after 1 year in the Pu-illite suspensions are also plotted in Figure 3a. According  
295 to these estimations, Pu(IV) is expected to prevail (or, at least, to be present in significant  
296 amounts) at the illite surface in all samples. For pH > 6, Pu(III) becomes negligible and Pu  
297 speciation in solution and at the illite surface is controlled by Pu(IV). For pH < 5, the overall Pu  
298 uptake by illite is predicted to lie between that of Eu(III) and Np(IV), which is indeed the case  
299 according to experimental data (Figure 3b).

300 We performed Eu(III) uptake experiments in 0.1 M NaCl ( $[\text{Eu}]_{\text{tot}} = 3 \times 10^{-9}$  M) for  $3 < \text{pH} < 9$  with  
301 our illite batch in order to exclude the possible impact of different clay mineral batches with

302 slightly variable surface properties (e.g. due to application of different purification procedures)  
303 on sorption. As shown in Fig. S2, the 2 SPNE SC/CE model with the set of surface complexation  
304 constants determined for Eu(III)<sup>19</sup> predicts the experimental data fairly well without any  
305 parameter adjustment. As discussed previously,<sup>13</sup> the estimated surface complexation constants  
306 for Np(IV) are based on various assumptions and affected by relatively large uncertainties (i.e. an  
307 error of  $\pm 1.1$  on log K values for the 2 SPNE SC/CE model) for various reasons and are  
308 restricted to  $4 < \text{pH} < 10$ . According to our pe measurements, only Pu(IV) is expected in solution  
309 for  $\text{pH} > 6$  after 1 year, as confirmed by Pu redox state analysis. According to our calculations, no  
310 redox state of Pu other than Pu(IV) should be present at the surface for  $\text{pH} > 6$ . We, therefore,  
311 conclude that our data are representative of the sorption behavior of Pu(IV) and that they can be  
312 used to derive more precise surface complexation constants for tetravalent Pu (Table S2). The  
313 respective constants lie below those reported earlier for Np(IV) but still within the uncertainty  
314 ranges (Figure S3). To describe Pu(IV) sorption at  $\text{pH} < 4$  (Figure 3b) we included the  
315  $\equiv\text{SOPuOH}^{2+}$  surface complex in order to be consistent with sorption data for other tetravalent  
316 cations (Th(IV)<sup>21</sup> and Sn(IV)<sup>20</sup>, see Figure S3) that do not exhibit a  $R_d$  decrease at  $\text{pH} < 4$  as is  
317 the case for simulated Np(IV) data. Results are shown as the blue line in Figure 3b. Applying  
318 those new surface complexation data in Table S2 does not result in major changes for the  
319 resulting  $\{\text{Pu(IV)/Pu(III)}\}_{\text{surf}}$  borderline (Figure 3a, bold red line). Our above conclusions remain  
320 valid.

321 Using the 2 SPNE SC/CE model with the surface complexation constants in Table S2 and taking  
322 into account the range of measured redox conditions ( $\text{pH} + \text{pe} = 11.8 \pm 1.0$ ; Figure. 3a) allows for  
323 an excellent simulation of experimental Pu sorption data over the whole pH-range investigated  
324 (Figure 2a). Decreasing  $R_d$  values at  $\text{pH} < 5$  are nicely reproduced as a consequence of  
325 progressing reduction of Pu(IV) to Pu(III) with decreasing pH. Variations in log  $R_d$  for  $\text{pH} = 4.3$

326 are assigned to the effect of  $pe$  rather than to a concentration effect (Fig. 2c). For  $6 < pe < 8.5$ ,  
327 Pu(III) prevails in solution whereas Pu(IV) prevails at the illite surface. This explains why  $\log R_d$   
328 values lie between that of Pu(III) and Pu(IV), when they occur as single components.

329

330 **Environmental implications.** These results related to Pu(IV)/Pu(III) transition in presence  
331 of illite, together with the outcome of earlier studies such as Pu(V)/Pu(IV) redox reactions in  
332 aqueous kaolinite suspensions<sup>17</sup> or the Np(V)/Np(IV) transition in presence of illite,<sup>13</sup>  
333 demonstrate the applicability of our approach to describe actinide redox reactions in presence of  
334 mineral surfaces over a wide range of possible redox conditions where Pu(III), Pu(IV) and Pu(V)  
335 may exist. A more accurate simulation of redox sensitive element behavior in near surface soil  
336 systems and deep geological formations becomes possible by implementing measured  $pe$  values  
337 of a given system into geochemical surface speciation calculations. Therefore, this study may  
338 allow a more accurate estimation of Pu mobility in the geosphere. Because natural systems can be  
339 much more complicated, containing e.g. carbonates and natural organic matter, further studies are  
340 required to verify the applicability of the present approach to a wider range of geochemical  
341 conditions. Our approach might also be tested for redox sensitive elements other than actinides  
342 (e.g. cerium, selenium, arsenic, chromium, iron).

343

#### 344 ASSOCIATED CONTENT

345 Materials and Methods: Extraction methods, Pu oxidation state analysis. Results and Discussion:  
346 Thermodynamic calculations (Surface complexation, cation exchange, SIT parameters),  
347 Experimental sorption data. This material is available free of charge via the Internet at  
348 <http://pubs.acs.org>.



349

350 **AUTHOR INFORMATION**

351 **Corresponding Author**

352 \* nidhu.banik@kit.edu

353

354 **Present Addresses**

355 †Ecole Nationale Supérieure de Chimie de Rennes, UMR CNRS 6226, 11 Allée de Beaulieu, F-  
356 35708 Rennes Cedex 7, France.

357 # Groupe d'Etudes Atomiques (GEA), Ecole des Applications Militaires de l'Energie Atomique  
358 (EAMEA). BCRM Cherbourg, CC19 50115 Cherbourg-Octeville Cedex, France

359

360 **Notes**

361 The authors declare no competing financial interest.

362

363 **ACKNOWLEDGEMENTS**

364 This work was financed by the Federal Ministry of Economic Affairs and Energy (Germany)  
365 under contracts No. 02E10206 and 02E10961. The research leading to these results has received  
366 funding from the European Union's European Atomic Energy Community's (Euratom) Seventh  
367 Framework Program FP7/2007-2011 under grant agreement n° 249624 (CATCLAY project).

368

369

370 **REFERENCES**

- 371 (1) Altmaier, M.; Gaona, X.; Fanghanel, T. Recent advances in aqueous actinide chemistry and  
372 thermodynamics. *Chemical Reviews* **2013**, *113* (2), 901-943.
- 373 (2) Geckeis, H.; Lutzenkirchen, J.; Polly, R.; Rabung, T.; Schmidt, M. Mineral-Water interface  
374 reactions of actinides. *Chemical Reviews* **2013**, *113* (2), 1016-1062.
- 375 (3) Begg, J. D.; Zavarin, M.; Zhao, P. H.; Tumey, S. J.; Powell, B.; Kersting, A. B. Pu(V) and  
376 Pu(IV) sorption to montmorillonite. *Environmental Science & Technology* **2013**, *47* (10), 5146-  
377 5153.
- 378 (4) Zavarin, M.; Powell, B. A.; Bourbin, M.; Zhao, P. H.; Kersting, A. B. Np(V) and Pu(V) ion  
379 exchange and surface-mediated reduction mechanisms on montmorillonite. *Environmental*  
380 *Science & Technology* **2012**, *46* (5), 2692-2698.
- 381 (5) Tinnacher, R. M.; Begg, J. D.; Mason, H.; Ranville, J.; Powell, B. A.; Wong, J. C.; Kersting,  
382 A. B.; Zavarin M. Effect of Fulvic Acid Surface Coatings on Plutonium Sorption and Desorption  
383 Kinetics on Goethite. *Environmental Science & Technology* **2015**, *49* (5), 2776–2785.
- 384 (6) Hixon, A. E.; Powell, B. A. Observed changes in the mechanism and rates of Pu(V) reduction  
385 on hematite as a function of total plutonium concentration. *Environmental Science & Technology*  
386 **2014**, *48* (16), 9255-9262.
- 387 (7) Powell, B. A.; Fjeld, R. A.; Kaplan, D. I.; Coates, J. T.; Serkiz, S. M. Pu(V)O<sub>2</sub><sup>+</sup> Adsorption  
388 and Reduction by Synthetic Magnetite (Fe<sub>3</sub>O<sub>4</sub>). *Environmental Science & Technology* **2004**, *38*,  
389 6016-6024.
- 390 (8) Powell, B. A.; Fjeld, R. A.; Kaplan, D. I.; Coates, J. T.; Serkiz, S. M. Pu(V)O<sub>2</sub><sup>+</sup> adsorption  
391 and reduction by synthetic hematite and goethite. *Environmental Science & Technology* **2005**, *39*  
392 (7), 2107-2114.

- 393 (9) Romanchuk, A. Y.; Kalmykov, S. N.; Aliev, R. A. Plutonium sorption onto hematite colloids  
394 at femto- and nanomolar concentrations. *Radiochimica Acta* **2011**, *99*, 137-144.
- 395 (10) Romanchuk, A. Y.; Kalmykov, S. N.; Egorov, A. V.; Zubavichus, Y. V.; Shiryayev, A. A.;  
396 Batuk, O. N.; Conradson, S. D.; Pankratov, D. A.; Presnyakov, I. A. Formation of crystalline  
397  $\text{PuO}_{2+x} \cdot n\text{H}_2\text{O}$  nanoparticles upon sorption of Pu(V,VI) onto hematite. *Geochimica et*  
398 *Cosmochimica Acta* **2013**, *121*, 29-40.
- 399 (11) Hixon, A. E.; Arai, Y.; Powell, B. A. Examination of the effect of alpha radiolysis on  
400 plutonium(V) sorption to quartz using multiple plutonium isotopes. *Journal of Colloid and*  
401 *Interface Science* **2013**, *403*, 105-112.
- 402 (12) Banik, N. L.; Buda, R. A.; Burger, S.; Kratz, J. V.; Trautmann, N. Sorption of tetravalent  
403 plutonium and humic substances onto kaolinite. *Radiochimica Acta* **2007**, *95*, (10), 569-575.
- 404 (13) Marsac, R.; Banik, N. L.; Lutzenkirchen, J.; Marquardt, C. M.; Dardenne, K.; Schild, D.;  
405 Rothe, J.; Diascorn, A.; Kupcik, T.; Schafer, T.; Geckeis, H. Neptunium redox speciation at the  
406 illite surface. *Geochimica et Cosmochimica Acta* **2015**, *152*, 39-51.
- 407 (14) Guillaumont, R.; Fanghänel, Th.; Fuger, J.; Grenthe, I.; Neck, V.; Palmer, D. A.; Rand, M.  
408 H. *Update on the Chemical Thermodynamics of Uranium, Neptunium, Plutonium, Americium and*  
409 *Technetium*; Amsterdam, **2003**.
- 410 (15) Kirsch, R.; Fellhauer, D.; Altmaier, M.; Neck, V.; Rossberg, A.; Fanghanel, T.; Charlet, L.;  
411 Scheinost, A. C. Oxidation state and local structure of plutonium reacted with magnetite,  
412 mackinawite, and chukanovite. *Environmental Science & Technology* **2011**, *45* (17), 7267-7274.
- 413 (16) Buda, R. A.; Banik, N. L.; Kratz, J. V.; Trautmann, N. Studies of the ternary systems humic  
414 substances – kaolinite – Pu(III) and Pu(IV). *Radiochimica Acta* **2008**, *96*, 657-665.

- 415 (17) Marsac, R.; Banik, N. L.; Lützenkirchen, J.; Buda, R. A.; Kratz, J. V.; Marquardt, C. M.  
416 Modeling plutonium sorption to kaolinite: Accounting for redox equilibria and the stability of  
417 surface species. *Chemical Geology* **2015**, *400*, 1-10.
- 418 (18) Choppin, G. R. Utility of oxidation state analogs in the study of plutonium behavior.  
419 *Radiochimica Acta* **1999**, *85*, 89-95.
- 420 (19) Bradbury, M. H.; Baeyens, B.; Geckeis, H.; Rabung, T. Sorption of Eu(III)/Cm(III) on Ca-  
421 montmorillonite and Na-illite. Part 2: Surface complexation modelling. *Geochimica*  
422 *Cosmochimica Acta* **2005**, *69*, 5403-5412.
- 423 (20) Bradbury, M. H.; Baeyens, B. Sorption modelling on illite Part I: Titration measurements  
424 and the sorption of Ni, Co, Eu and Sn. *Geochimica et Cosmochimica Acta* **2009**, *73* (4), 990-  
425 1003.
- 426 (21) Bradbury, M. H.; Baeyens, B. Sorption modelling on illite. Part II: Actinide sorption and  
427 linear free energy relationships. *Geochimica et Cosmochimica Acta* **2009**, *73* (4), 1004-1013.
- 428 (22) Marquardt, C. M.; Seibert, A.; Artinger, R.; Denecke, M. A.; Kuczewski, B.; Schild, D.;  
429 Fanghanel, T. The redox behaviour of plutonium in humic rich groundwater. *Radiochimica Acta*  
430 **2004**, *92*, (9-11), 617-623.
- 431 (23) Nitsche, H.; Roberts, K.; Xi, R. H.; Prussin, T.; Becraft, K.; Almahamid, I.; Silber, H. B.;  
432 Carpenter, S. A.; Gatti, R. C.; Novak, C. F. Long-Term plutonium solubility and speciation  
433 studies in a synthetic brine. *Radiochimica Acta* **1994**, *66-7*, 3-8.
- 434 (24) Neck, V.; Altmaier, M.; Seibert, A.; Yun, J. I.; Marquardt, C. M.; Fanghanel, Th. Solubility  
435 and redox reactions of Pu(IV) hydrous oxide: Evidence for the formation of  $\text{PuO}_{2+x(\text{s,hyd})}$ .  
436 *Radiochimica Acta* **2007**, *95*, 193-207.
- 437 (25) Kinniburgh, D. G., Cooper, D. M. *PhreePlot: Creating graphical output with PHREEQC*.  
438 <http://www.phreeplot.org>. **2009**.

- 439 (26) Parkhurst, D. L.; Appelo, C. A. J. *User's guide to PHREEQC (Version 2) – a computer*  
440 *program for speciation, batch reaction, one-dimensional transport and inverse geochemical*  
441 *calculation*; Denver, Colorado, **1999**; PP 312.
- 442 (27) Ciavatta, L. The specific interaction theory in evaluating ionic equilibria. *Annali Di Chimica*  
443 **1980**, 70, (11-1), 551-567.
- 444 (28) Gorgeon, L. Contribution à la modélisation physico-chimique de la rétention de  
445 radioéléments à vie longue par des matériaux argileux. *Ph.D. thesis, Université Paris 6, 1994*.
- 446 (29) Farr, J. D.; Neu, M. P.; Schulze, R. K.; Honeyman, B. D. Plutonium uptake by brucite and  
447 hydroxylated periclase. *Journal of Alloys and Compounds* **2007**, 444, 533-539.
- 448 (30) Bauer, A.; Berger, G. Kaolinite and smectite dissolution rate in high molar KOH solutions at  
449 35° and 80°C. *Applied Geochemistry* **1998**, 13, 905-916.
- 450 (31) Rabung, T.; Pierret, M. C.; Bauer, A.; Geckeis, H.; Bradbury, M. H.; Baeyens, B. Sorption  
451 of Eu(III)/Cm(III) on Ca-montmorillonite and Na-illite. Part 1: Batch sorption and time-resolved  
452 laser fluorescence spectroscopy experiments. *Geochimica Cosmochimica Acta* **2005**, 69, 5393-  
453 5402.
- 454 (32) Finck, N.; Schlegel, M. L.; Bosbach, D. Sites of Lu(III) Sorbed to and Coprecipitated with  
455 Hectorite. *Environmental Science & Technology* **2009**, 43 (23), 8807-8812.
- 456 (33) Bradbury, M. H.; Baeyens, B. Predictive sorption modelling of Ni(II), Co(II), Eu(III),  
457 Th(IV) and U(VI) on MX-80 bentonite and Opalinus Clay: A “bottom-up” approach. *Applied*  
458 *Clay Science* **2011**, 52, 27-33.
- 459 (34) Marques Fernandes, M; Vér, N.; Bart Baeyens, B. Predicting the uptake of Cs, Co, Ni, Eu,  
460 Th and U on argillaceous rocks using sorption models for illite. *Applied Geochemistry* **2015**, 59,  
461 189-199.

462 (35) Kalmykov, S. N.; Vlasova, I. E; Romanchuk, A. Y.; Zakharova, E. V.; Volkova, A. G.;  
463 Presnyakov, I. A. Partitioning and speciation of Pu in the sedimentary rocks aquifer from the  
464 deep liquid nuclear waste disposal. *Radiochimica Acta* **2015**, *103* (3), 175-185.  
465

466 **Figure Caption**

467 **Figure 1.** pH-pe values measured in illite suspensions under anaerobic conditions. Present work:  
468 1 week (gray diamonds) and 1 year equilibration time (black diamonds); previous investigations  
469 of the Np-illite system: white circles.<sup>13</sup> Large symbols indicate the samples where the supernatant  
470 was analyzed by liquid extraction ( $[\text{Pu}]_{\text{tot}} = 10^{-8}$  M). The predominance pH-pe diagram for Pu in  
471 0.1 M NaCl (solid lines) is also shown.

472 **Figure 2.** (a) Pu sorption to illite ( $R_d$ : distribution coefficient in  $\text{L kg}^{-1}$ ) in 0.1 M NaCl as a  
473 function of the pH ( $8 \times 10^{-11} < [\text{Pu}]_{\text{tot}} < 10^{-8}$  M) after 1 week (white squares) and 1 year (black  
474 diamonds) contact time. Results after 1 year are compared with overall  $\log R_d$  calculated for pH +  
475 pe =  $11.8 \pm 1.0$  (bold line; lower and upper values: dashed and dashed-dotted lines, respectively;  
476 see text for more details). (b) log-log plot of  $R_d$  versus the final aqueous Pu concentration ( $[\text{Pu}]_{\text{aq}}$ )  
477 for pH = 4.3 (black triangles) and pH > 5 (gray circles) after 1 year contact time. Average value  
478 and standard deviation of  $\log R_d$  ( $5.2 \pm 0.2$ ) for pH > 5 are shown as gray solid and dashed lines,  
479 respectively. (c) Experimental and calculated  $\log R_d$  values for pH = 4.3 versus pe.

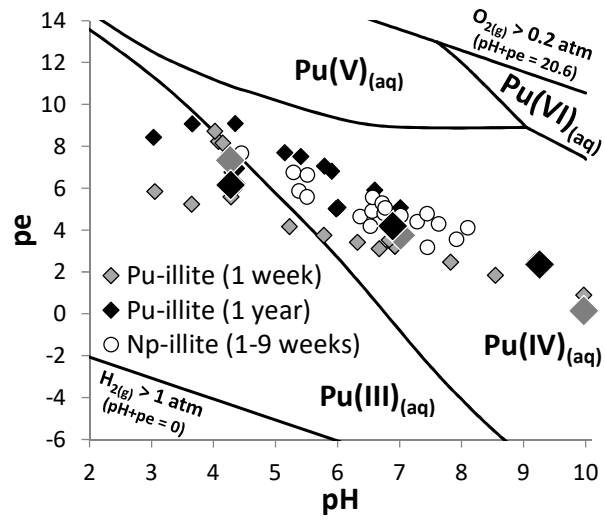
480 **Figure 3.** (a) Predominance pH-pe diagram for Pu in 0.1 M NaCl with pH-pe values measured in  
481 illite suspensions after 1 year equilibration time. The bold and dashed red lines show estimated  
482 borderlines for Pu(IV)/Pu(III) redox transition at the illite surface (see text for more details).  
483 Relevant redox conditions for this study (pH+pe =  $11.8 \pm 1.0$ ) are shown as straight (solid and  
484 dashed) lines. (b) Data for Pu uptake onto illite ( $R_d$  in  $\text{L kg}^{-1}$ ) as a function of pH compared with  
485 model calculations for Eu(III) (green bold line), Np(IV) (dashed black line) and Pu(IV) (blue  
486 bold line) sorption based on the 2 SPNE SC/CE model.

487

488

489

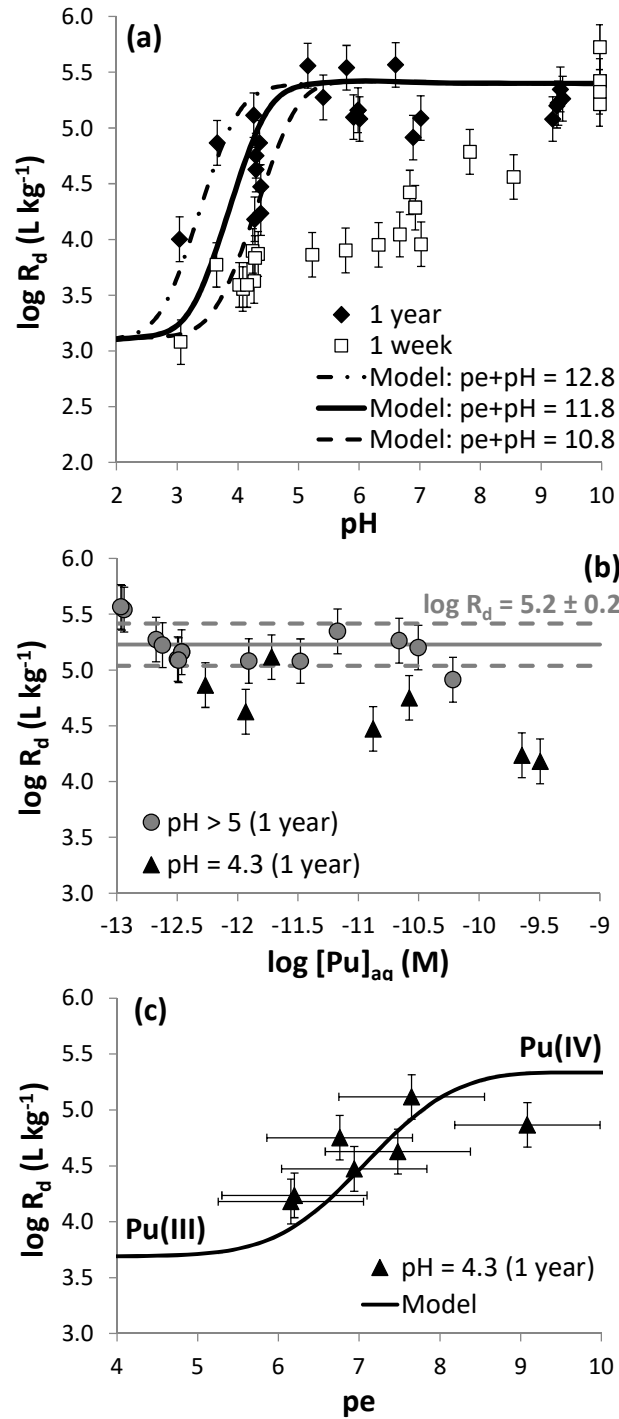
Figure 1



490

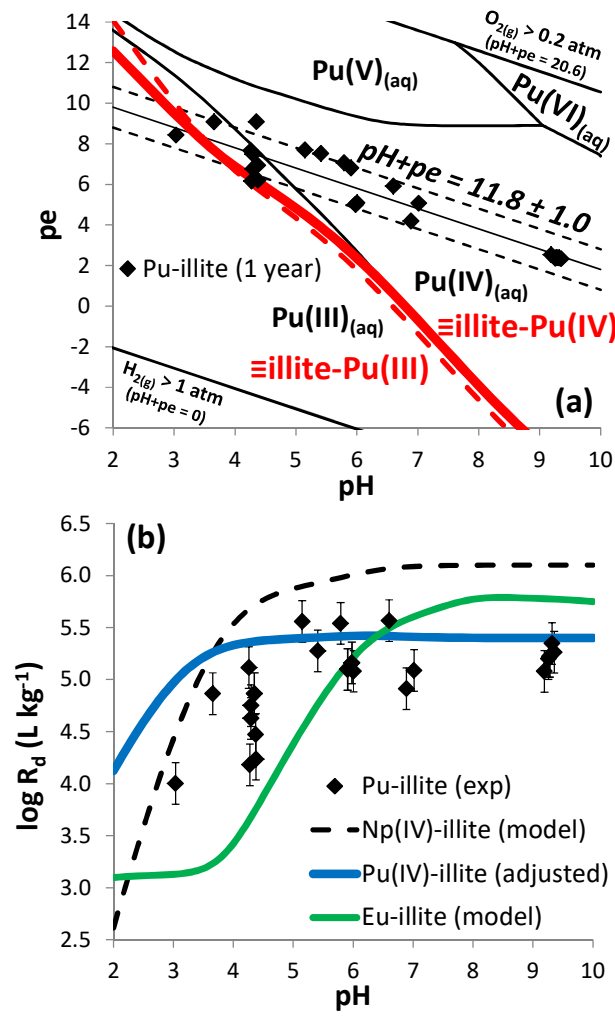


Figure 2



493

Figure 3



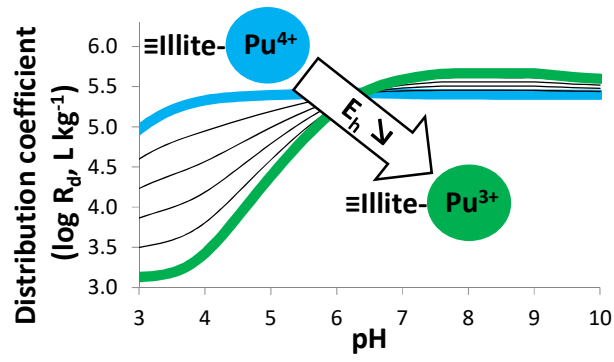
494

495

496

497

### TOC/abstract



498